AFRL-RH-WP-TR-2014-0143

ORGAN-ON-A-CHIP FOR AEROSPACE PHYSIOLOGY AND TOXICOLOGY

Joshua E. Smith
Christin M. Grabinski
Laura K. Stolle
The Henry M. Jackson Foundation

Andrew M. Sarangan
University of Dayton

Trevor B. Tilly
Oak Ridge Institute for Science and Education

Jennifer A. Martin
UES, Inc.

Saber M. Hussain
Molecular Bioeffects Branch

Claude C. Grigsby
Human Signatures Branch

DECEMBER 2014
Interim Report

AIR FORCE RESEARCH LABORATORY
711TH HUMAN PERFORMANCE WING
HUMAN EFFECTIVENESS DIRECTORATE
WRIGHT-PATTERSON AIR FORCE BASE, OH 45433
AIR FORCE MATERIEL COMMAND
UNITED STATES AIR FORCE

NOTICE AND SIGNATURE PAGE

Using Government drawings, specifications, or other data included in this document for any purpose other than Government procurement does not in any way obligate the U.S. Government. The fact that the Government formulated or supplied the drawings, specifications, or other data does not license the holder or any other person or corporation; or convey any rights or permission to manufacture, use, or sell any patented invention that may relate to them.

This report was cleared for public release by the 88th Air Base Wing Public Affairs Office and is available to the general public, including foreign nationals. Copies may be obtained from the Defense Technical Information Center (DTIC) (http://www.dtic.mil).

AFRL-RH-WP-TR-2014-0143 HAS BEEN REVIEWED AND IS APPROVED FOR PUBLICATION IN ACCORDANCE WITH ASSIGNED DISTRIBUTION STATEMENT.

//signature//

Claude C. Grigsby, Ph.D.
Work Unit Manager
Human Signatures Branch

//signature//

Louise A. Carter, Ph.D.
Chief, Human-Centered-ISR Division
Human Effectiveness Directorate
711th Human Performance Wing
Air Force Research Laboratory

This report is published in the interest of scientific and technical information exchange, and its publication does not constitute the Government's approval or disapproval of its ideas or findings.

REPORT DOCUMENTATION PAGE

Form Approved
OMB No. 0704-0188

1. REPORT DATE *(DD-MM-YY)*	2. REPORT TYPE	3. DATES COVERED *(From - To)*
15 12 14	Interim	12/18/2013-12/17/2014

4. TITLE AND SUBTITLE
Organ-on-a-Chip for Aerospace Physiology and Toxicology

5a. CONTRACT NUMBER
In-House

5b. GRANT NUMBER

5c. PROGRAM ELEMENT NUMBER

6. AUTHOR(S)
Joshua E. Smith[1], Christin M. Grabinski[1], Laura K. Stolle[1], Andrew M. Sarangan[2], Trevor B. Tilly[3], Jennifer A. Martin[4], Saber M. Hussain[5], Claude C. Grigsby[6]

5f. WORK UNIT NUMBER
H04V (7184C002)

7. PERFORMING ORGANIZATION NAME(S) AND ADDRESS(ES)
[1]The Henry M. Jackson Foundation
6720A Rockledge Drive, Suite 100
Bethesda MD 20817
[2]University of Dayton
[3]Oak Ridge Institute
[4]UES, Inc.
[5]Molecular Bioeffects Branch
[6]Human Signatures Branch

8. PERFORMING ORGANIZATION REPORT NUMBER

9. SPONSORING/MONITORING AGENCY NAME(S) AND ADDRESS(ES)
Air Force Materiel Command
Air Force Research Laboratory
711th Human Performance Wing
Human-Centered ISR Division
Human Signatures Branch
Wright-Patterson Air Force Base, OH 45433

10. SPONSORING/MONITORING AGENCY ACRONYM(S)
711 HPW/RHXB

11. SPONSORING/MONITORING AGENCY REPORT NUMBER(S)
AFRL-RH-WP-TR-2014-0143

12. DISTRIBUTION/AVAILABILITY STATEMENT
Distribution A: Approved for public release; distribution is unlimited

13. SUPPLEMENTARY NOTES
88ABW-2015-0757; Cleared 02 March 2015

14. ABSTRACT
The relationship between physiological stressors and the mechanisms of imposed changes at the cellular level is vital knowledge to mitigate injury of armed forces personnel from chemical or environmental exposures. Current batch cell culture models are unable to recapitulate the conditions experienced in a dynamic *in vivo* microenvironment, where nutrients are constantly circulating and waste is removed. Additionally, animal exposure models are costly and time-consuming, and often fail to accurately predict human outcomes. We completed proof of concept work on a biomimetic model that more reliably portrays *in vivo* conditions by designing a microfluidic biomimetic lung exposure model that can be used in place or as an initial screening mechanism prior to animal studies for assaying chemical and environmental exposure. This approach adapts current microfluidic technology for novel Aerospace toxicology investigations specific to volatile compounds. We developed in-house microfluidic fabrication capabilities, design and create organ-chip devices with *in vivo* mimetic traits, establish microfluidic cell culture methods and assays of rat lung cells. With the fabrication techniques demonstrated, this work serves as the foundation for the development of a biomimetic rat lung model. This model could serve as a low-cost, screening template enabling the rapid transition of the technology to assess emerging materials, operational environments, and toxic threats to the DoD community with further device validation.

15. SUBJECT TERMS
microfluidics, biomimetic, organ on a chip, cell culture, toxicity, toxicological, genetic, metabolomic

16. SECURITY CLASSIFICATION OF:			17. LIMITATION OF ABSTRACT:	18. NUMBER OF PAGES	19a. NAME OF RESPONSIBLE PERSON (Monitor)
a. REPORT	b. ABSTRACT	c. THIS PAGE			Claude Grigsby, Ph.D.
U	U	U	SAR	29	19b. TELEPHONE NUMBER *(Include Area Code)*

THIS PAGE IS INTENTIONALLY LEFT BLANK.

TABLE OF CONTENTS

LIST OF FIGURES

ACKNOWLEDGEMENT

This work was funded by the 711 Human Performance Wing Chief Scientist Office as part the seedling program.

1.0 INTRODUCTION

Humans are increasingly exposed to environmental conditions exerting stress on various aspects of their physiology. Military personnel endure an especially high risk to stressors in a deployed setting with potential exposures to toxic chemicals, chemical and biological warfare agents, radiological threats, and physiological extremes due to aerospace operations. These stressors often result in changes at the cellular level, manifesting in morphological, toxicological, genetic, and metabolomic variances measurable with current technology. Understanding this relationship between environmental insult and physiological response is a crucial component towards preventing injury and maintaining the safety of our operators. Therefore, our goal was to complete proof of concept on a novel method of studying these various changes, i.e morphologic, genetic, metabolomic, to identify markers of stress using a biomimetic cellular exposure model.

Current models of exposure rely heavily on cell culture. This traditional model investigates cells cultured in a 2-dimensional (2D) layer on a cell culture plate. However, this environment fails to accurately portray the dynamics of a 3-dimensional (3D) microenvironment where the circulatory system is constantly providing a fresh supply of nutrients and removing the resulting metabolic waste (Huh, Hamilton et al. 2011). This waste build-up imposes environmental stress on the cells, making it challenging to differentiate whether detected physiological responses are due to the artificial cellular environment or the intentional insult initiated by the researcher. Scientists have attempted to address this issue through creation of *biomimetic* models, or systems inspired by nature, to more accurately reflect *in vivo* conditions. In the instance of cell culture, 3D cell culture models are emerging as a technology wherein cells are cultured on fabricated devices engineered to mimic tissue microarchitecture (Huh, Hamilton et al. 2011). These models are cultured within an extracellular matrix (ECM) shown to increase expression of differentiated cell function and improved cellular organization relative to 2D cell culture. In this model, nutrients exposed to the biomimetic tissue layer will diffuse through the cellular matrix creating a gradient of nutrient contact much like those experienced *in vivo* (Huh, Torisawa et al. 2012).

Some of the most promising biomimetic models are the result of combining 3D cell cultures with microfluidic fabrication technology. Microfluidic technology enhances biomimetic models by enabling a controlled, continuous flow of nutrients and metabolic waste removal at a natural scale close to that of mammalian systems (10-100 μm), with precisely defined liquid to cell volume ratios (Esch, King et al. 2011). Scientists have also successfully modeled tissue-tissue interfaces similar to those conditions observed *in vivo* (Huh, Matthews et al. 2010). For example, the microvascular endothelium and surrounding parenchymal tissues interact to transport fluids, nutrients, immune cells and other regulatory factors between the two layers. Microfluidic devices have been designed to have a porous membrane where endothelial and specific parenchymal cells of interest to a particular organ are grown on opposite sides of the membrane to recreate these dynamics. In addition, microfluidic technology enables simulation of the dynamic forces experienced in the cellular microenvironment that 2D models cannot reproduce. Some examples include the shear stress imposed on cells by fluid flow, fluid resistance times, and cell stretching effects from the breathing motion (Esch, King et al. 2011, Huh, Hamilton et al. 2011).

Several groups have produced work highlighting the benefits of microfluidic 3D cell culture models for organs including the liver, lung, kidney, gut, bone, and heart. Applying chemical gradients as experienced by individual cells within tissue samples, and incorporating representative dynamic cues have produced cells with a more differentiated, normal phenotype compared to standard 2D models (El-Ali, Sorger et al. 2006, Whitesides 2006). Huh and collaborators have shown that a biomimetic lung model replicated complex organ level responses to bacteria and cytokines, a result not previously observed in a reported cell culture system. This group used high-resolution microscopy to visualize expression of intercellular adhesion molecule-1, adhesion of circulating neutrophils and transmigration across the tissue-tissue interface, and phagocytosis of pathogens (Huh, Matthews et al. 2010, Huh, Torisawa et al. 2012). This group also successfully demonstrated that the cyclic strain imparted to simulate the breathing motion in the lung model exacerbates toxicity and inflammation of the lung from nanoparticles relative to cells unexposed to cyclic strain. This result was subsequently confirmed in a whole mouse lung model, demonstrating that the biomimetic lung model more closely mimicked the *in vivo* results of animal studies (Huh, Torisawa et al. 2012).

Building upon on these findings, we completed preliminary design of a biomimetic microfluidic lung model as a screening method for physiological changes experienced as a result of chemical and environmental insult toward the goal of reducing reliance on animal models. Animal models are costly, time-consuming, and typically require a large sample size to produce statistically significant results. In addition, ethical considerations surrounding animal use are always a concern, especially when animal studies are frequently unsuccessful in predicting a response in humans (Huh, Torisawa et al. 2012). Figure 1 (below) shows the concept in practice, where preliminary *in vitro* assays traditionally lead to animal models. Biomimetic organs such as the lung model may enable the researcher to save time and costs by providing a screening mechanism, by running biomimetic challenges in parallel to animal studies, or ideally replacing animal models altogether. The ultimate goal of biomimetic organ study is to integrate all organs onto a single microcirculatory system platform ("biomimetic body") to recapitulate the physiology of exposure to organs and blood in a dynamic, sequential process. By linking the organ models, a more accurate depiction of *in vivo* physiology occurs, with processes such as metabolism, clearance, and/or immune response represented in succession.

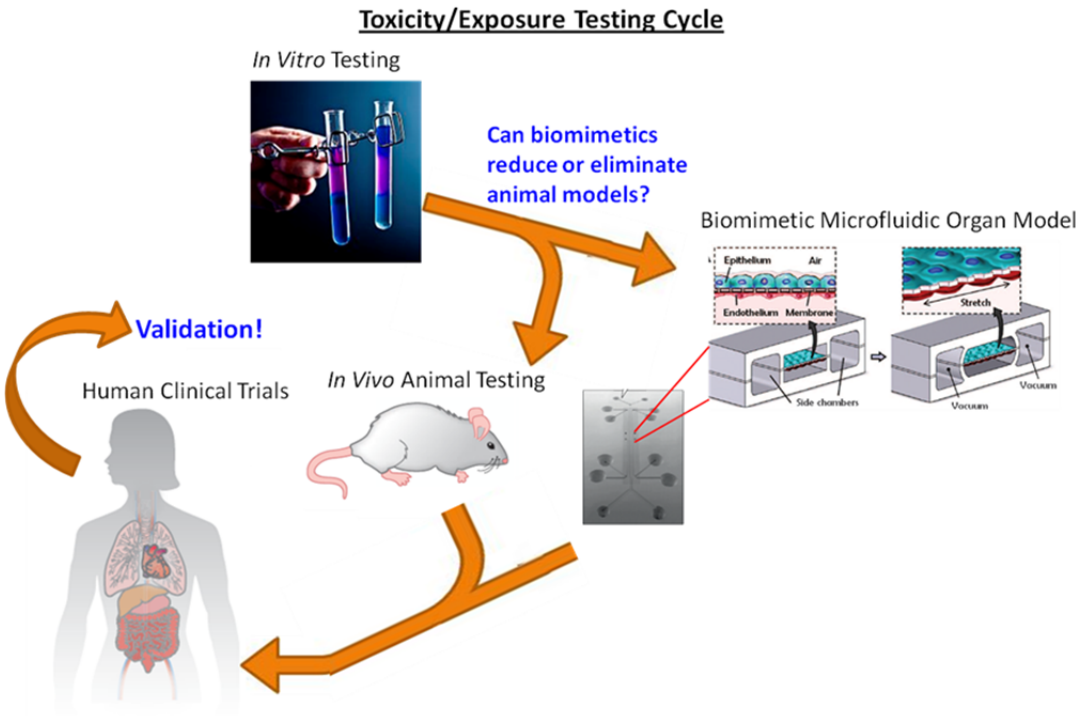

Figure 1: Proposed Toxicity/Exposure Testing Cycle
will incorporate biomimetic microfluidic organs (biomimetic lung pictured from Huh, Trends in Cell Biology, 2011) as a method to reduce reliance on animal models.

Inhalation models are especially important following recent reports of hypoxia-like symptoms experienced by pilots of high performance aircraft. The effects of hypoxia can severely degrade a pilot's ability to operate aircraft, and may include light-headedness, fatigue, or hallucinations. High performance aircraft pilots experiencing emergencies in-flight also reported loss of memory and/or confusion extending hours to days following the flight event. Additionally, pilots in high performance aircraft are also exposed to changes in altitude and subsequent variations in the supplied oxygen percentage ($\%O_2$) to prevent hypoxia. For example, modern fighters are capable of reaching an altitude of over 50,000 ft above sea level, where the cabin is pressurized to 20,000 ft. Due to the low partial pressure of O_2, the On-Board Oxygen Generation System (OBOGS) is on a schedule to concentrate the oxygen from roughly 60% at 10,000 ft to over 95% at 50,000 ft to mitigate occurrence of hypoxia. The effects of VOC exposure at altitude and varying oxygen levels are poorly understood characteristics, and may have a significant impact on physiology. Understanding the OBOGS schedule and how the oxygen levels affect health is crucial as both too little oxygen (hypoxia) and too much oxygen (hyperoxia) can result in a significant cognitive performance decline in pilots.

In summary, the goal of this work is to decrease the overall costs and experimental time required for physiological and toxicological screening through generation of a validated biomimetic model as an option to *in vivo* testing for aerospace assessment. This could be accomplished through development of microfluidic biomimetic organ models as a replacement for animal models. Herein, we have initiated in-house microfluidic device fabrication capabilities, and demonstrated the ability to fabricate the microfluidic based biomimetic platform. Furthermore, we utilized commercially available microfluidic devices to establish cell culture methods for multiple cell lines, and demonstrated the use of cellular stain assays. With further development,

this work could provide details on the simulated cellular microenvironment, establish exposure protocols, and validate the biomimetic model with animal studies. Establishment of this type of biomimetic model for physiological and toxicological screening could provide a new, adaptable tool for use in assessing the safety of United States Air Force (USAF) personnel that can be rapidly applied to numerous operational concerns in a constantly evolving defense environment.

2.0 MATERIALS AND METHODS

2.1 Reagents

All chemicals and reagents were purchased from Sigma-Aldrich (St. Louis, MO) unless otherwise indicated. Polydimethylsiloxane (PDMS), Sylgard 184 Silicone Elastomer Kit, Dow Corning was acquired from Fisher Scientific (Pittsburgh, PA). Buffered Oxide Etch (BOE), 50:1 NH_4F:HF was purchased from J.T. Baker Avantor Performance Materials (Center Valley, PA). SU-8 2100 and 2050 Photoresist, SU-8 developer, and cyclopentanone were obtained from MicroChem Corp. (Westborough, MA).

2.2 Equipment

All the equipment was purchased from Fisher Scientific (Pittsburgh, PA) unless otherwise indicated. The IMN1-LC linear channels 100 μm x 500 μm, standard IMN2 Idealized Co-culture construct, 500 ft of 0.02" ID x 0.06" OD Tygon® tubing, Open Jaw Slide Clamps, 24 Gauge Blunt Economical 0.5" Needles were obtained from SynVivo (Huntsville, AL). WS-650Mz-23NPPB and WS400-LITE Spin Processors were purchased from Laurell Technologies Corporation (North Wales, PA). The Expanded Plasma Cleaner, 115 V was acquired from Harrick Plasma (Ithaca, NY). A 22.8 x 30.4 x 22.8 cm Economy Vacuum Oven, Shel Lab was purchased from VWR (Randor, PA). Electro-Technic Products (Chicago, IL) supplied the Laboratory Corona Treater. Silicon wafers, 3" with <100> orientation were obtained from Wafer World Incorporated (West Palm Beach, FL). An Olympus CKX41 inverted microscope with a DP71 Charged Coupled Device (CCD) camera was procured from B and B Microscope (Pittsburgh, PA). The O_2 Plasma Chamber was reconditioned. The Misto olive oil sprayer (Atomizing sprayer) was purchased from Bed Bath and Beyond. Flat surface hot plate was obtained from Brewer Science (Rolla, MO).

2.3 Fabrication of SU-8 Silicon Masters and Silanization

The designs for the micro-channels (200 micron channel width) and porous membrane (50 micron diameter pores) were generated using Autodesk Inventor software (San Rafael, CA). The designs were converted into two dimensional Mylar® photo plots with a resolution of 50,800 dots per inch by Fineline Imaging (Colorado Spring, CO). Digital images are shown below in Figure 2:

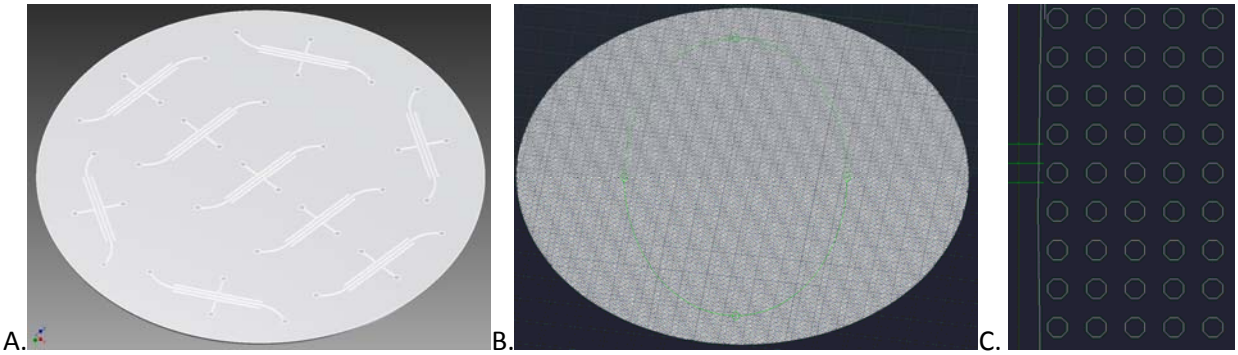

Figure 2: Digital Images of the Chip Design

A. single channel device with parallel channels on either side for cyclic vacuum suction to mimic breathing; B. porous membrane; C. magnified image of the porous membrane.

The silicon wafer was first immersed in the Buffered Oxide Etch (BOE) solution for approximately one minute to etch the old native oxide. Timing was not critical, but the surface becoming hydrophobic verifies the complete removal of the oxide. The wafer was then rinsed in deionized water and dried with nitrogen. The wafer was then placed in the oxygen plasma chamber to reoxidize and activate the surface. The chamber was pumped down to a base pressure of about 100 mT, and pure O_2 gas was flowed at a process pressure of 500 mT. The plasma was ignited at discharge power of 250 W at 30 kHz and allowed to run for 1 minute. The wafer was then removed, and quickly moved to a work table in a dark room (with Ultra-Violet (UV) filtered lights) where the SU-8 photoresist was applied. The plasma activated surface can accumulate ambient moisture and this will affect the adhesion of the SU-8 to silicon, so this step needed to be done quickly. The SU-8 2100 or 2050 photoresist was spread on the surface of the wafer with a small metal spatula. The exact quantity or uniformity was not critical at this point, but it needed to cover at least 2/3 of the wafer surface. Then the wafer was transported to a spin coater and placed on the vacuum chuck. The spin speed was set to 1500 Revolutions per Minute (RPM) and run for 60 seconds. Following the spin coating, with the wafer still on the vacuum chuck, the edges and backside of the wafer was carefully wiped with an acetone towel to remove any residual SU-8 to prevent the wafer from becoming glued to the hotplate in the next step.

The coated wafer was then transported to a gravity leveled hot plate. A small quantity of cyclopentanone was placed into the pressurized atomizing sprayer. While holding the sprayer about 12 inches from the wafer the sprayer was activated for 2-3 seconds to produce a mist that gently settles on the wafer. There has to be adequate ventilation for safety, but excessive ventilation can prevent the mist from settling on the wafer. The goal was to produce a thin uniform meniscus of cyclopentanone on top of the SU-8. Bubbles and blisters that were on the original SU-8 surface should start to dissipate within a few seconds after the application of the cyclopentanone. Then the hot plate was turned on for a slow ramp of 2-deg/min to reach a peak temperature of 100 ˚C, followed by a slow ambient cooling back to room temperature (which for this hot plate took two to three hours). The wafer was typically left on the hotplate overnight, and was covered with a dark petri dish to prevent exposure to light.

The photomask which contains the SU-8 design was installed on the mask aligner in preparation for UV exposure. In this setup, an inexpensive photoplotted image on a mylar sheet was attached to a blank glass plate with isopropyl alcohol. The UV exposure unit contains a 1000-Watt

mercury vapor lamp. An acrylic sheet was placed on top of the mask to filter out the 365 nm emission line and allow the 405 nm and 436 nm lines because the high absorption coefficient of 365 nm in SU-8 can produce undesired sidewall tapers. The exposure was set to deliver a dose of 2.1 J/cm^2 (30 mW/cm^2 for 70 seconds) using a soft-contact mode for the SU-8 2100. The exposure time was decreased to 60 sec for the SU-8 2050. Following the exposure, the wafer was retrieved and placed on the gravity level hotplate again for the post-exposure bake. The same ramp and cool parameters as before were followed. Slow ramps are more critical for the post-exposure bake as stress cracks can emerge in the cured SU-8. The bake was typically done during an overnight period.

The exposed and cured wafer was then immersed in a beaker with the SU-8 developer solution to dissolve the unexposed areas of the SU-8, for approximately 10-15 minutes with occasional mild agitation. The pattern development should become clearly visible. Then the wafer was removed from the beaker and thoroughly rinsed in isopropyl alcohol, and dried with a nitrogen gun. The SU-8 pattern was subsequently inspected on an optical microscope.

Before the SU-8 can be used as a stamp, a release agent has to be applied so that the PDMS will not permanent bond to the SU-8 or the silicon wafer surface. This was done by placing the wafer in a petri dish and drop casting a sufficient quantity of Sigmacote to cover the entire wafer surface. The wafer was allowed to sit in the fluid for about 1 minute, and then it was rinsed off in deionized water. The Sigmacote made the wafer surface hydrophobic which can be seen during the rinse. Then the wafer was dried. This completed the stamp fabrication process. This silane treatment method was attempted for both the microchannel and membrane wafer.

Additional silane treatment methods for the membrane wafer included the vapor deposition of hexamethyldisiloxane (HMDS) in a vacuum chamber. The process for applying a thin layer of HMDS is very sensitive to ambient moisture. Hence, the sample is first dehydrated in a vacuum oven with temperature and the introduction of dry nitrogen. First, the sample is placed in the oven heated to 100 C. Then a vacuum is drawn down to 10 Torr, followed by refilling the chamber to 500 Torr with dry nitrogen. This pump-purge cycle is repeated three times. Then a base vacuum is drawn down to 100 mT. Then the HMDS valve is opened to release the vapor. The vapor pressure of HMDS at room temperature (since the HMDS bottle is kept at room temperature outside of the heated chamber) is 6 Torr. The pressure in the chamber will therefore rise to 6 Torr and become stable. This pressure is held for the desired exposure time, typically 5 to 10 minutes. For the membrane wafer, the exposure time was performed overnight. Following the HMDS exposure, the pump and N_2 purge cycles are repeated three more times. This time the purpose is to remove all traces of the HMDS vapor. Then the chamber was vented with N_2 up to atmospheric pressure and the sample is retrieved.

Vapor deposition of trichloro(1H,1H,2H,2H-perfluorooctyl)silane (TPS) was performed at room temperature overnight in a vacuum desiccator. The membrane wafer was placed in the desiccator a long side two adjacent glass slides and 4 drops of TPS were placed on each glass slide. The desiccator was evacuated to maximum vacuum, the vacuum vent was closed, and the samples left overnight.

2.4 Fabricating the PDMS Microchannels

In a disposable container, 15 g of the elastomer base from the Sylgard 184 Kit was massed on a balance by using a 20 mL disposable syringe. To the container, 1 g of curing agent from the Sylgard184 Kit was added with a disposable pipette. The sample was mixed with a Teflon

spatula until the PDMS appeared white, typically 5-10 minutes. The developed silicon wafer patterned with the microchannels was placed in a 100 mm Petri dish. The prepared PDMS sample was transferred to the Petri dish, and placed in a vacuum desiccator to remove air bubbles from the uncured PDMS mixture, typically around 30 minutes. To cure the PDMS, the Petri dish was transferred to a hot plate that was set at 60 ˚C for five hours or the Petri dish was left overnight at room temperature and placed on a hot plate set at 60 ˚C for one hour. After curing, the dish was removed from the hot plate and allowed to cool to room temperature.

The PDMS was cut along the edge of the silicon wafer using a scalpel, and peeled from the surface of the wafer, which resulted in the replicate mold of the microchannels. These molds were then cut to size and shape. The fluidic and vacuum access ports were bored using a 1.5 mm biopsy punch. Note: these ports were bored on the micropatterned side of the cured PDMS to ensure proper alignment of the ports with the microchannels. Both sides of the devices were covered with packing tape for storage and removed when ready for bonding (see description below). The tape also served to clean the PDMS surface prior to use.

2.5 Microchannel-Glass Slide Bonding

Microchannel slabs were bonded to glass slides through plasma treatment of the surfaces. Plasma treatment of the glass slide and PDMS channel surfaces was performed one of two ways. Either using a handheld corona tool operated in a chemical safety hood or the PDMS slabs were treated inside a barrel shaped plasma chamber. For the handheld tool, the PDMS surface was treated with plasma by sweeping the apparatus over the slabs or glass slide for 90 seconds. In the barrel chamber, the PDMS surface and glass slide were treated with plasma for 60 seconds. The chamber operation was as follows: place materials for plasma treatment on the quartz shelf, close the chamber door, switch on the power supply, turn on the vacuum pump, wait for the chamber to achieve maximum evacuation, open the air valve, and slowly increase the radio frequency (RF) level to high. After the 60-second treatment, the RF was slowly switched off, the air valve was closed, the vacuum pump was switched off, and the chamber was vented to the atmosphere. After plasma treatment, the channel was placed on the glass slide, and the materials were placed on a hot plate set at 85 ˚C for 5-10 min to complete the bonding process.

2.6 Fabrication of the PDMS Membrane

A 2” x 3” glass slide was treated with Sigmacote as a silanizing agent through direct application to the glass surface. The silanizing agent allows for the release of the cured PDMS from the glass surface. The slide was rinsed with deionized water and dried with compressed nitrogen. The glass slide was placed in a 100 mm Petri dish. A 20 g mixture of 15:1 Sylgard 184 base to curing agent was poured into the Petri dish. Air bubbles were removed from the uncured PDMS in a vacuum desiccator. The PDMS was cured on a hot plate, as described above. After cooling to room temperature, the PDMS slab was cut along the edge of the glass slide with a scalpel, and peeled from the glass slide surface. Then the slab was cut into 2.5 cm x 4 cm rectangular blocks using a scalpel. Again, the PDMS block was covered with packing tape until used. The tape served to prevent the deposition of dust during storage and served to clean the PDMS block prior to use.

When ready, the tape was removed and the surface of the PDMS block was silane treated. A variety of silane treatment methods were attempted. This was done to find the optimal treatment condition. The details of the treatment processes are described in a later section. A thin layer of uncured PDMS was pin coated onto the PDMS block. For the spin coating process, the PDMS

block was placed on a Sigmacote treated glass slide, and placed on a vacuum chuck of the spin coater. The uncured PDMS was prepared by mixing a 10:1 ratio of PDMS base to curing agent in a disposable container. Air bubbles were removed by placing the container is a vacuum desiccator for ~ 30 minutes. With a disposable pipette, the PDMS mixture was transferred to the silanized PDMS block. The spin coater was ramped at 500 RPMs/sec to a final speed of 2000 RPMs. This speed was maintained for 60 seconds. The uncured PDMS film and block was placed on the silicon wafer array that contained the SU-8 generated membrane pillars. A 200 g mass was placed on the glass slide to allow for pillar penetration into the uncured PDMS film. The sample was left at room temperature overnight, and final curing was performed by heating on a hot plate at 60 ˚C for one hour. The material was carefully peeled from the silicon wafer surface. The membrane-block has the ability to be stored in this manner until needed.

2.7 PDMS Block, Silane Treatment

The PDMS block treatment was performed with a variety of methods. Initial silane treatments were performed with a standard silanizing agent, Sigmacote. The first attempt employed the vapor deposition of 4-5 drops of the silane applied to a glass slide that was placed in a vacuum desiccator (Treatment I). The PDMS block was placed adjacent to the silane treated glass slide, and the vacuum applied. Once the desiccator reached maximum evacuation, the pump was turned off and the samples were left overnight. A more aggressive treatment was to apply the silane directly to the PDMS block, and rinse the surface with deionized water after several minutes (Treatment II). This treatment provided a more intact transfer of the membrane compared to the previous attempt. A final Sigmacote process used an excess of the silanizing agent in vacuum chamber, as described in the first attempt. However, with this attempt, the entire glass slide was covered with ~1-1.5 mL of silane (Treatment III). This approach provided the most aggressive treatment with the Sigmacote agent by providing the most intact membrane transfer.

HMDS treatment of the PDMS block was performed in the same manner as the silicon wafer treatment. Exposure of the PDMS block was performed in a temperature controlled vacuum chamber. Two different block exposure times were used, overnight and 30 minutes. The overnight treatment was performed at 100 ˚C for the duration of the PDMS block treatment (Treatment IV). The 30 minutes exposure was done at room temperature (Treatment V). A third silanizing agent, TPS, treatment of the PDMS block was attempted. This treatment was performed in the vacuum desiccator for overnight, two hours or 30-minute exposure times (Treatments VI, VII, and VIII). Additional explanations and details regarding these exposure conditions are provided in the Results Section.

2.8 Assembly of Multilayer Device

Both channel-on-channel (two-layer) and membrane containing (three-layer) devices were assembled. To fabricate the two-layer device, two PDMS cast channel molds were plasma treated, and the channels aligned for assembly using an optical microscope with a 4x objective and a long working distance. Plasma treatment was performed as described previously. The assembled devices were placed on a hot plate set at 85 ˚C for 5-10 minutes to complete the bonding process. For the three-layer device, plasma treatment of one channel and the membrane were performed as described. Then the membrane-block was set on the channel surface. The assembled materials were placed on a hot plate (85 ˚C) for 5-10 minutes to complete the bonding process. The membrane block was slowly peeled from the channel bonded membrane to

complete the membrane transfer. The channel-membrane and a second channel were plasma treated as described. Again, the two sets of channels were aligned using an optical microscope, and the assembly was placed on a hot plate (85 ˚C) for 5-10 minutes.

2.9 Cell Culture

Synvivo linear channel devices with 500 μm wide channels were cultured with three rat cell types. First, the lung macrophage immune cell line, NR8383, was used in the device. The NR8383 cell line prefers an extracellular matrix for attachment, and there was difficulty getting the cells to adhere in the device, due to their mobile cell nature. The second cell type used was the adrenal gland cell line, PC-12, which is an adherent cell type that was adapted from suspension. The PC-12 cells were used to determine if cells would adhere in the microfluidic device, after difficulty with the macrophages. Finally, the rat lung epithelial cell line, L2 (American Type Culture Collection, ATCC), was cultured in the microfluidic devices. Prior to seeding in the devices, the cells were grown in 75 cm^2 culture treated flasks in an incubator at 37 ºC and 95% relative humidity to 80% confluence. When ready, 2 mL of 0.5% trypsin was used to detach the cells from the tissue culture flask.

Three different types of media were required for the three cell types. For the NR8383 cells, Dulbecco's modified Eagle medium supplemented with 10% fetal bovine serum and 1% penicillin/streptomycin. Ham's F12 Media with 15% horse serum, 2.5% fetal bovine serum, and 1% penicillin/streptomycin was the culture media for the PC-12 cells. Ham's F-12 Medium with 10% fetal bovine serum and 1% penicillin/streptomycin was used as the L2 cell growth media.

2.10 Coating Microfluidic Device for Cell Culture

Rat tail fibronectin and collagen were the two extracellular matrices were utilized to coat the microfluidic devices for cell culture. Rat tail extracellular matrices were selected to avoid species specific preference of the L2 cell line. Fibronectin or collagen was injected into the devices at a concentration of 100 μg/mL or 50 μg/mL, respectively, and then the devices were placed in the incubator overnight. Excess extracellular matrix was flushed from the device with L2 cell growth media the following morning, and at least 4 hours was allowed to elapse before cells were seeded into the device.

2.11 Cellular Seeding in the Microfluidic Devices

Cells were rinsed twice with 2 mL of 0.5% trypsin, and then 2 mL of trypsin was added for 10 minutes. Once the cells detached, they were pipetted up and down no less than 20 times, and then counted using a vision cellometer by Nexcelom Bioscience. The cells were then centrifuged at 1000 Relative Centrifugal Units (RCF) for 5 minutes. The supernatant was aspirated, and then the necessary amount of media was added to produce a cell concentration between 20-50 $*10^6$ cells/mL.

The cells were kept at 37 ºC using a hotplate until they were seeded into the microfluidic devices. When ready, a pre-coated device was placed and focused on an Olympus IX71 Microscope. A water droplet was added to each of the inlet ports, and the inlet tubing was removed using forceps. A 1 mL syringe with tubing already attached was filled with the L2 cell solution, and then the tubing was inserted into the device. The microscope was used to visualize the seeding, and once a good concentration was achieved, the tubing was cut and clamped.

2.12 Cell Viability

The cell viability in the device was measured by the LIVE/DEAD Cell Viability Assay from Life Technologies. The manufacturer protocols were adapted from the manufactures protocols for small volumes. The cells after staining were visualized using the Olympus IX71 Microscope.

3.0 RESULTS AND DISCUSSION

The motivation for this project was to establish the capability to manufacture microfluidic devices in-house. With that goal, we were able to procure the equipment and gain the knowledge necessary to design and fabricate single and multilayer devices. The following sections describe the processes used in the assembly and evaluation of the biomimetic and simple microchannel based device fabrication.

3.1 Chip Master Fabrication and Silane Treatment

The SU-8 fabrication process has been well-developed in our laboratory over a number of years, so the application method, exposure parameters and bake steps did not require much experimentation. The image shows one of the fabricated SU-8 stamp on a three-inch silicon wafer (Figure 3). The thickness of thee SU-8 was measured to be approximately 120-130 μm. This was measured with a mechanical micrometer since it was beyond the maximum range of our stylus profilometer.

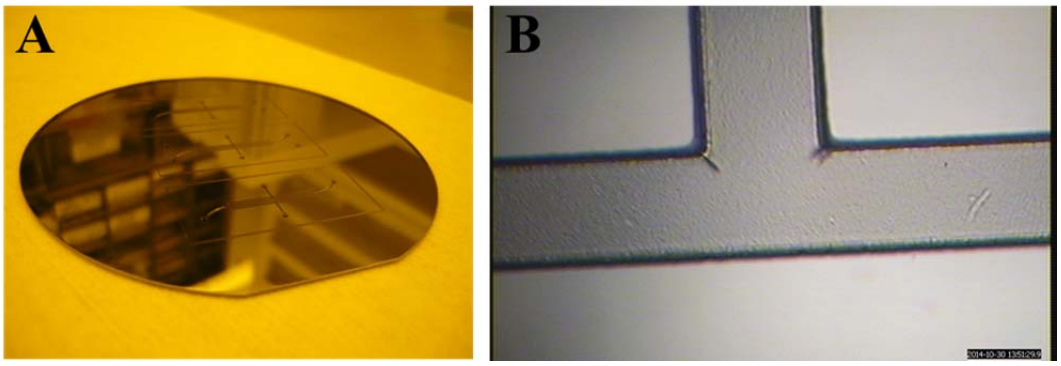

Figure 3: SU-8 Patterned Microfluidic Device Channels
A) Left is the photo image and B) right is a microscope image.

The microscope image shows that the sidewalls of the SU-8 were reasonably vertical and do not show any tapers. The beginnings of stress cracks were also seen at the corners. These are fairly typical with thick SU-8 films, and are due to shrinkage as the SU-8 becomes cross-linked during the post-exposure bake. The same process and analysis was performed with the membrane patterned silicon wafer (see photo images below).

The purpose of the Sigmacote was to make the SU-8/silicon a very low-energy surface so that PDMS will not permanently adhere to it. Sigmacote treatment worked well as a release agent for the microchannel patterned wafers. However, Sigmacote treatment of the silicon wafer proved to be too mild for the effective release of the membrane from the wafer surface, which is evident by the residual PDMS left on the wafer (Figure 4A). The residual PDMS was not able to be cleaned from the wafer, even with solvent washes (ie: acetone, isopropanol, or heptane). The main issue here was that the wafer surface was unusable after a single use, and the membrane wafer needed to be continually fabricated. Therefore, more aggressive silane treatment for the wafer was investigated. Newly fabricated membrane wafers were treated with either HMDS or TPS. HMDS treatment did provide an improved release of the PDMS from the membrane wafer (Figure 4B). After two-to three repeat uses, the surface was unusable and additional wafers needed to be fabricated. With the TPS treated membrane wafers, these wafers were continually

reused. The surface was cleaned by gentle wiping to remove the remaining cured PDMS material (Figure 4C).

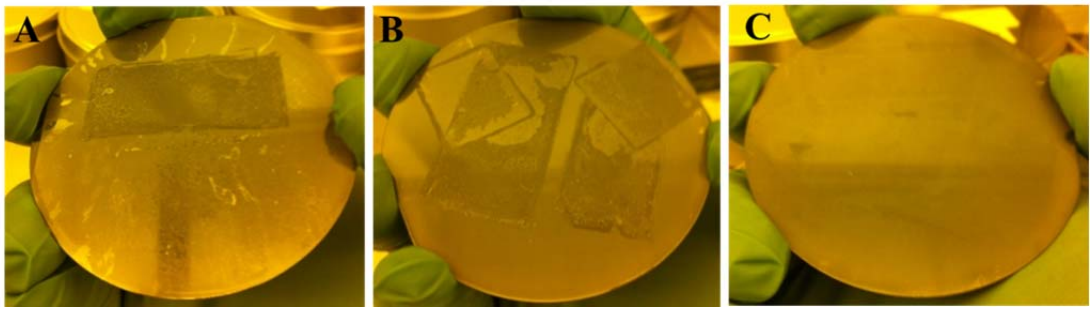

Figure 4: Silcon Wafer membrane Stamp after Release of the PDMS Membrane and Cleaning Process
A) Sigmacote, B) HMDS, and C) TPS

3.2 Microfluidic Device Fabrication-On Glass Slides, Two-Layer Device, and Three-Layer Device

Each organ chip section (microchannels and membrane) was first attached to a glass slide. This was done to evaluate the condition of each of the individual device pieces. For the micro-channels, the device access ports and channels were imaged with an optical microscope. This was done after plasma bonding the PDMS molded channels to a glass slide (Figure 5). The evaluation was performed to ensure that the channel walls were not deformed and access port holes were successfully aligned following the boring step. The bonded channels were filled with a blue dye to ensure that device bonding was achieved. This was evident by way of the dye residing in the device channels and that no dye leakage was observed.

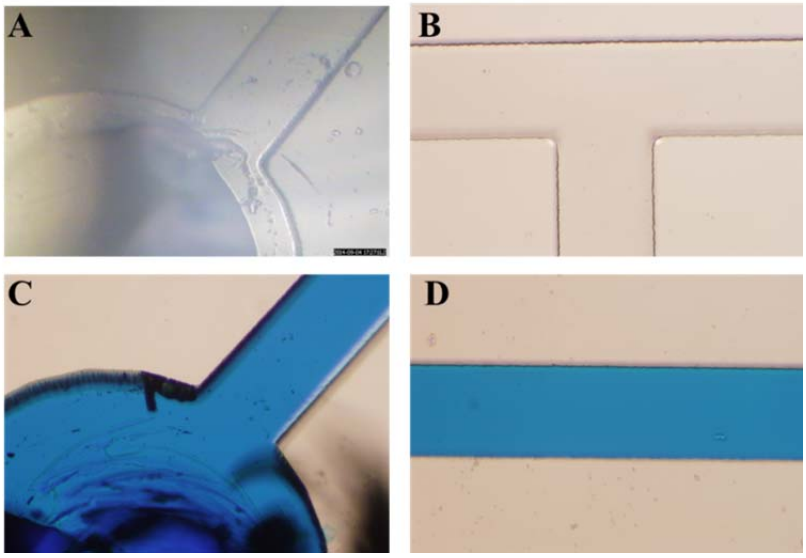

Figure 5: Microfluicic Device Channels and Ports after Plasma Bonding to a Glass Slide
A) Device port, B) device channel, C) device port filled with dye, and D) device channel filled with dye

For the membrane, it was transferred to a glass slide, as described. After removal of the PDMS block, images of the material were obtained with an optical microscope (Figure 6). With the initial investigations, the determination was made that the silane treatment of the silicon membrane wafer and the PDMS block used in the membrane fabrication process were critical steps for the success of this process. A delicate balance between an aggressive wafer silane treatment and a more mild PDMS block treatment was desired. This was evident by the degree at which the membrane was released from the silicon wafer, and the extent that the membrane transferred to the glass slides. For the membranes displayed in Figure 6A-C, the silicon wafer was treated with Sigmacote and each of the PDMS-blocks were treated with more aggressive treatment protocols. The more aggressive block treatments (Figure 6B and C) resulted in a better transfer of the membrane to the glass slide, Treatments II and III respectively. The membranes transferred to glass were determined to be 15-25 μm thick.

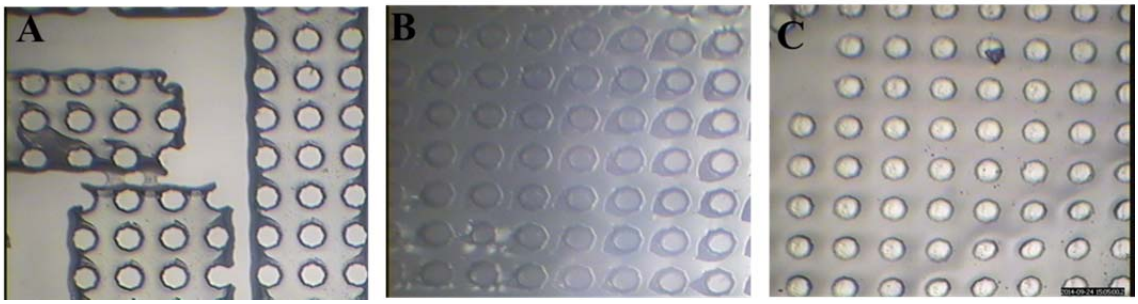

Figure 6: Porous Membranes Transferred to Glass Slides
A) Treatment I, B) Treatment II, and C) Treatment III

The fabrication of two-layer devices was performed, as described. Figure 7 displays the channel-on-channel two-layer device assembly. The channel alignment was performed with an optical microscope, and the devices were imaged after completing the bonding process. Figure 7A and D shows the two-layer device filled with blue dye to demonstration the integrity of the device bonding with no apparent leaking observed from the channels. Microscope images of the two-layer device are displayed in Figure 7B and C, which confirms the successful alignment of the two microchannel replicate molds.

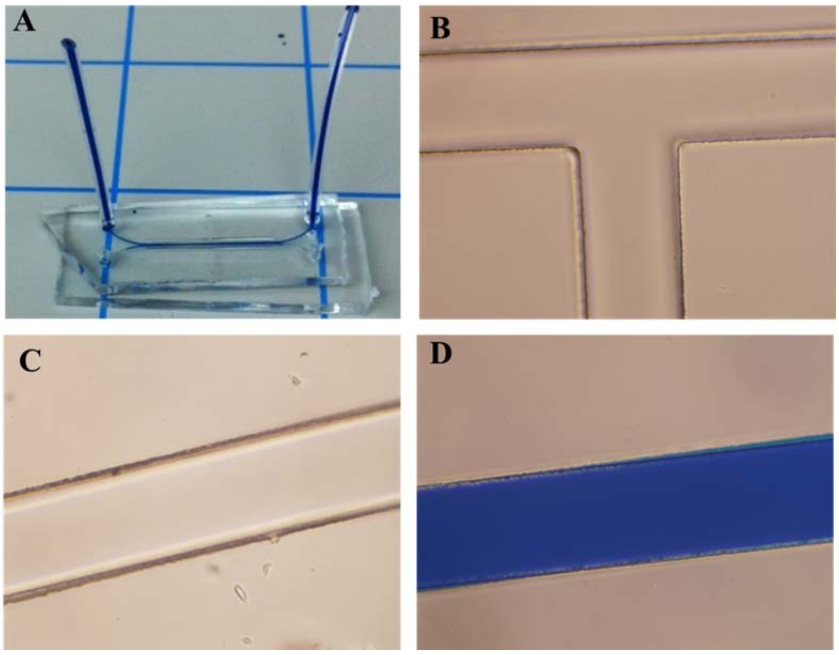

Figure 7: Plasma Bonded Two-Layer Device

A) Photo of dye filled device, B and C) microscope images of bonded device, and D) microscope image of dye filled device

A three-layer device (lung chip) was fabricated, as described. Figure 8 represents the assembly process used to create the membrane containing lung chip device. Details regarding the fabrication and transfer of the PDMS membrane are in the next section. When fabricating the lung chip, channel alignment was performed with an optical microscope. Device images were obtained after the completion of each of the apparatus bonding steps. Figure 8B and C show the microscope images of the bonded membrane to a single microchannel and the completed three-layer device, respectively. These images confirm the successful alignment of the microchannels. While Figure 8A and D represent the three-layer device filled with dye. The channel and device bonding integrity were demonstrated with no apparent leaking observed from the channels.

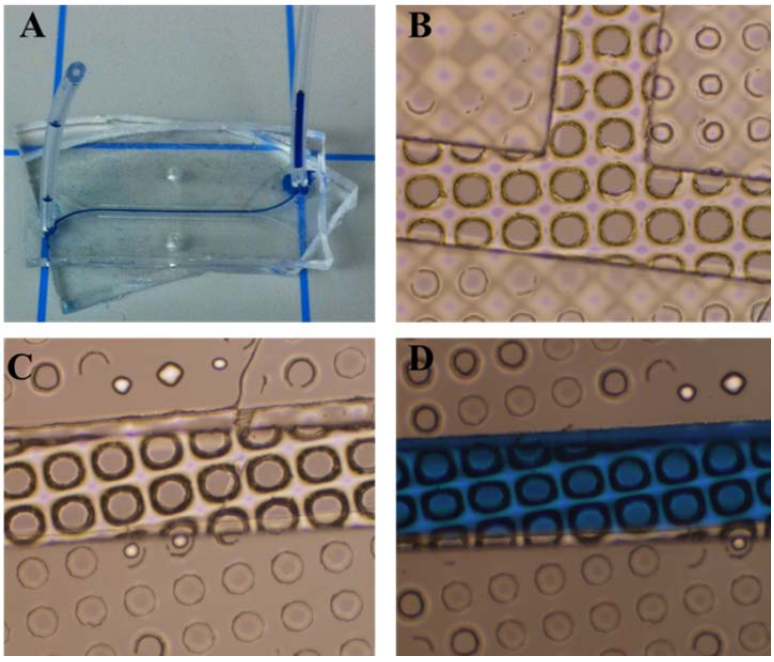

Figure 8: Plasma Bonded Membrane Containing Devices
A) Photo of dye filled device, B) microscope image of membrane on channels C) microscope image of 3-layer device, and D) microscope image of dye filled 3-layer device

3.3 Membrane-Channel Transfer

Regarding transfer of the membrane to the channels, the Sigmacote treatments provided a poor release mechanism from the PDMS block. The membrane was torn from the channel leaving the channel exposed in all the Sigmacote protocols. This data combined with the silicon wafer treatment indicated that a more aggressive silane treatment for the PDMS block was preferred. HMDS treatment of the silicon wafer was more aggressive than the Sigmacote. Therefore, HMDS treatment was performed with the PDMS block, Treatments IV and V. Unfortunately, these protocols resulted in PDMS blocks that were brittle and disintegrated during the membrane transfer step.

This lead to treating the PDMS block with the TPS protocols, Treatments VI-VII. At this point, the silicon wafer was treated exclusively with the TPS protocol. Treatment VI was too aggressive for the PDMS block. The membranes generated on these blocks were unsuccessfully released from the TPS treated wafer. The PDMS block was completely clean and had no membrane on the surface. The overnight treatment of the block proved to be too aggressive. A less aggressive treatment was desired for the PDMS block, Treatment VII. This membrane was used in the fabrication of the three-layer device described above. However, the membrane was not completely detached, intact from the silicon wafer. This membrane was successfully transferred to the channel (see previous section).

Based on the results for Treatment VII, Treatment VIII was performed to improve the membrane release from the stamp. This method provided a shorter silane exposure time than the previous treatment, which resulted in a milder silane block treatment. Unfortunately, the transfer of the membrane to the channel was unsuccessful. The channels remained exposed after bonding the membrane to the channel. Further optimization is needed for this process.

3.4 Cell Seeding and Characterization

Three cell lines were tried in the Synvivo linear channel devices. The cell type was found to determine the successfulness of the cells in the device. Figure 9 shows a comparison of cells during seeding, and after a 12-hour attachment period.

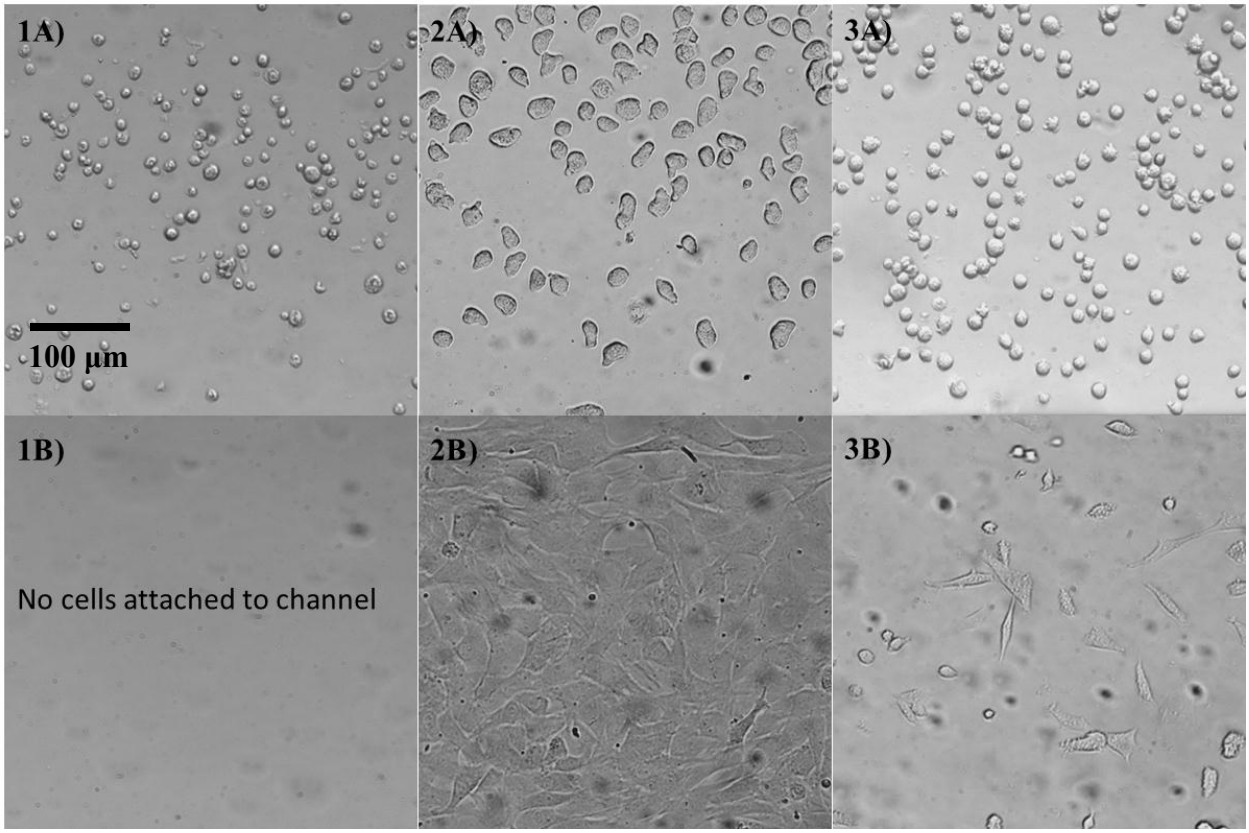

Figure 9: Cellular Seeding

(A) and attachment (B) of rat cell lines in the SynVivo linear channel device. The three cell lines shown are (1) lung macrophage NR8383, (2) lung epithelial L2, and (3) adrenal gland PC-12

There were differences in the size of the various cell types, and the levels of their attachment. The L2 cell size in suspension was significantly greater than the NR8383 and PC-12 cells. Both the PC-12 and the L2 cells stretched and attached in the channel. The L2 cells almost completed a monolayer in the channel, which can be seen in Figure 10B. No macrophage cells were observed in the channel after 12 hours of attachment. The L2 cell line was selected to be used in all of the future studies because of its success in the device.

The cell viability in the microfluidic devices was visualized through fluorescent staining, and visualization using a fluorescence microscope. Figure 10 shows a bright-field image and fluorescence image of the L2 cells after preparation of the LIVE/DEAD assay.

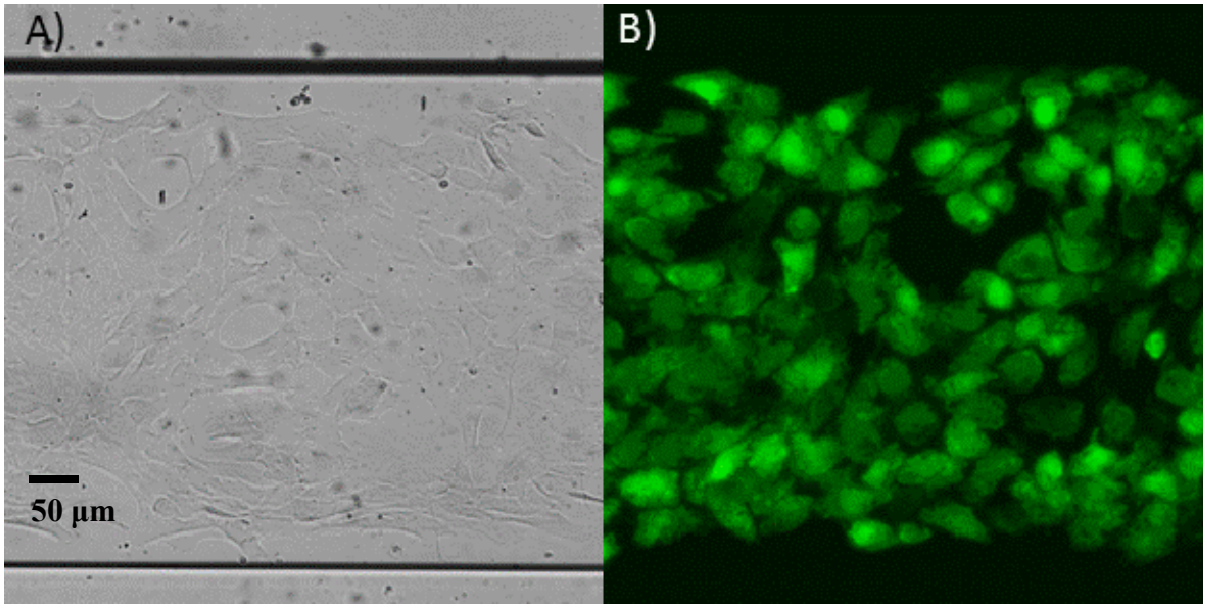

Figure 10: Visualization of L2 Lung Epithelial Cells in the Channel

Epithelial cells were grown successfully in the microfluidic devices, as can be seen in Figure 10. The LIVE/DEAD cell assay verified that the cells attaching in the channels of the Synvivo devices were alive. Additionally, from the bright-field and fluorescence images in Figure 10, it can be seen that the channels appear to be almost entirely confluent with the L2 cell type.

4.0 CONCLUSIONS

The primary purpose of this work was to acquire the capacity to design and fabricate microfluidic devices in-house. We obtained the equipment and knowledge necessary for fabrication. In this work, the microdevices were designed to incorporate a flexible PDMS membrane film for cellular culture support, which was sandwiched between two microchannels. This membrane allows the cells to experience peristaltic motion similar to *in vivo* microenvironments. Additionally, the microfluidic channels permit the continuous introduction of nutrients, removal of waste products, and facilitate shear forces cells experience *in vivo*.

For the fabrication of the devices, the microchannel and membrane chip masters were produced using photolithography techniques, including photo plots, silicon wafers, photoresists and micropatterned photomasks. The plots were generated from two dimensional digital models of the device components. The chip masters were used in the replicate mold stamping to fabricate the individual device components. The membrane and microchannel layers were assembled using plasma bonding. Microscope images of the master molds and produced devices were obtained to ensure chip and device integrity. In summary, we have demonstrated the fabrication techniques necessary to manufacture and assemble co-culture cellular platforms with desired biomimetic features. Cell culture and assay methods for microchannel platforms were also established.

To continue this project, the following improvements to the processes described here are recommended. The main issue with producing the organ chips was with the fabrication and incorporation of the thin membrane film. Issues with the consistent release of the PDMS film from the membrane stamp persisted throughout these investigations. The optimization of the silane treatment of both the PDMS block and the membrane wafer would need to be achieved. Additionally, the pore size and spacing should be adjusted to reflect the pore density and film quality of the published results. In the literature, a 1:4 pore size to spacing ratio was used. For these investigations, the pore size and spacing used was 50 μm and 100 μm, respectively, which increased the pore density by 2x. An increased pore density may compromise the membrane integrity by reducing the amount of PDMS material present. Furthermore, a higher pore density may increase the interactions between the membrane film and the silicon stamp, which could make release of an intact membrane more difficult.

Also for the preparation of the membrane, producing thicker PDMS cast blocks would be desired. With the PDMS recipe used, the blocks were quite thin, making them very flexible, and difficult to work with. Increasing the PDMS mass to ≥ 25 g would provide a thicker cast block, which will be easier to work with. In addition, the spin conditions require further process optimization to attain the desired membrane thicknesses. This work focused on reproducing the membranes described in the literature, but a study into the membrane thickness and design would be of interest to further advance the organ-chip technology. Specifically, a parametric study investigating the effect of pore size, pore density and membrane thickness on the ability for cells to form a confluent layer and access nutrients through the membrane would allow for the optimization of membrane properties for more facile fabrication.

Additional concern for the membrane stamping and release process is that it is susceptible to trapped air. A potential solution to this issue would be to perform the stamping process in a vacuum environment. This can be done with a vacuum wafer bonding system using a wafer bonder (e.g. Suss Microtech SB6L). Although designed for bonding two wafers, the same

process can be used for stamping uncured PDMS to the membrane wafer. The equipment contains two sandwiching plates. The top plate can move in the vertical axis, while the bottom plate is held fixed. Both plates are heated and can be adjusted to any desired temperatures, together or at different temperatures. The samples are mounted to these plates, and the chamber is closed. Then a vacuum is drawn inside the chamber. During this time the samples are held separate. Then the top plate is moved downwards to make contact with the bottom plate. The contact pressure and the distance of the movement can be accurately controlled. This way the two surfaces can be brought into contact without any air becoming trapped at the gaps. Following contact, the temperature can be increased to promote curing.

Likewise, improvements for the microchannels are needed. The greatest challenge observed was with the alignment of the channels in the multilayer manufacturing of the devices. This includes the boring and aligning of the channel access ports for the bottom layer. The redesign of the channel master wafer will provide guides for uniform device cutting and boring the ports through the top layer to provide access for the bottom channel, which will ease the challenge of manufacturing multilayer devices. Furthermore, producing thicker PDMS cast channels are desired. With the PDMS recipe used, the channels were thin, making them very flexible, and difficult to assemble into a layered device. Increasing the PDMS mass to $\geq$ 20 g would provide a thicker cast channel, which will be easier to work with.

Once successful, reproducible fabrication of the organ chips is achieved, the cell seeding and evaluation assay methods could be optimized to provide the groundwork for growing a variety of cell lines in biomimetic cell culture devices.

5.0 REFERENCES

El-Ali, J., P. K. Sorger and K. F. Jensen (2006). "Cells on Chips." *Nature* **442**(7101): 403-411.

Esch, M., T. King and M. Shuler (2011). "The Role of Body-on-a-Chip Devices in Drug and Toxicity Studies." *Annual Review of Biomedical Engineering* **13**: 55-72.

Huh, D., G. A. Hamilton and D. E. Ingber (2011). "From 3D Cell Culture to Organs-on-Chips." *Trends in Cell Biology* **21**(12): 745-754.

Huh, D., D. C. Leslie, B. D. Matthews, J. P. Fraser, S. Jurek, G. A. Hamilton, K. S. Thorneloe, M. A. McAlexander and D. E. Ingber (2012). "A Human Disease Model of Drug Toxicity–Induced Pulmonary Edema in a Lung-on-a-Chip Microdevice." *Science Translational Medicine* **4**(159): 159ra147-159ra147.

Huh, D., B. D. Matthews, A. Mammoto, M. Montoya-Zavala, H. Y. Hsin and D. E. Ingber (2010). "Reconstituting Organ-Level Lung Functions on a Chip." *Science* **328**(5986): 1662-1668.

Huh, D., Y.-s. Torisawa, G. A. Hamilton, H. J. Kim and D. E. Ingber (2012). "Microengineered Physiological Biomimicry: Organs-on-Chips." *Lab on a Chip* **12**(12): 2156-2164.

Whitesides, G. M. (2006). "The Origins and the Future of Microfluidics." *Nature* **442**(7101): 368-373.

6.0 LIST OF ACRONYMS

2D	Two-Dimensional
3D	Three-Dimensional
BOE	Buffered Oxide Etch
CCD	Charged Coupled Device
DoD	Department of Defense
ECM	Extracellular matrix
HMDS	Hexamethyldisiloxane
ID	Inner Diameter
OBOGS	On-Board Oxygen Generation System
OD	Outer Diameter
PDMS	Polydimethylsiloxane
RF	Radio Frequency
RPM	Revolutions per Minute
TPS	Trichloro(1H,1H,2H,2H-perfluorooctyl) silane
USAF	United States Air Force
UV	Ultra-Violet
VOC	Volatile Organic Compound